ELSEVIER

Journal of Organometallic Chemistry 560 (1998) 223–232

Journal of Organometallic Chemistry

Preparations and structures of (η^6-arene)ruthenium(II) complexes bearing 1,1′-bis(diphenylphosphinomethyl)ferrocene or 1,1′-bis(diphenylphosphino)ferrocene

Jian-Fang Mai [1], Yasuhiro Yamamoto *

Department of Chemistry, Faculty of Science, Toho University, Miyama, Funabashi, 274, Japan

Received 16 December 1997; received in revised form 3 February 1998

Abstract

Reactions of bis[dichloro(η^6-arene)ruthenium] **1** with 1,1′-bis[(diphenylphosphino)methyl]ferrocene (dpmf) gave the dpmf-*P*,*P*′ bridged complexes [(η^6-arene)$RuCl_2$]$_2$(μ-dpmf) **2**, where arenes = (**a**) 1,2,3,4-$Me_4C_6H_2$; (**b**) C_6Me_6; (**c**) *p*-cymene; (**d**) 1,2,3,5-$Me_4C_6H_2$; (**e**) 1,3,5-$Me_3C_6H_3$; (**f**) 1,2,3-$Me_3C_6H_3$. Treatment of **2** with xylyl isocyanide (XylNC) in the presence of $NaPF_6$ produced the F-coordinated complex [(η^6-arene)RuCl]$_2$(μ-dpmf)$(PF_6)_2$ **3a** without containing XylNC. Reactions of **1** with 1,1′-bis(diphenylphosphino)ferrocene (dppf) formed the bridged complexes [(arene)$RuCl_2$]$_2$(μ-dppf)] **4**, as well as the dpmf complexes. The similar reactions in the presence of $NaPF_6$ gave the chelated complexes [(η^6-arene)RuCl(dppf-*P*,*P*′)](PF_6) **5**. Crystal structures of **2a**, **2d**·$2CH_2Cl_2$, **4a**·CH_2Cl_2 and **5b** were confirmed by X-ray analyses and they have three-legged piano-stool structures. Crystal data are as follows: **2a** triclinic, space group $P\bar{1}$, with $a = 12.802(6)$, $b = 19.111(6)$, $c = 11.438(4)$ Å, $\alpha = 98.93(3)$, $\beta = 108.57(3)$, $\gamma = 90.42(3)°$, $V = 2615(1)$ Å^3, $Z = 2$ [$R = 0.051$, $R_w = 0.052$ for 4114 independent reflections with $I > 3.0\sigma(I)$]; **2d**·$2CH_2Cl_2$ monoclinic, space group $C2/c$, $a = 38.379(6)$, $b = 9.903(3)$, $c = 17.381(4)$ Å, $\beta = 113.91(1)°$, $V = 6038$ Å^3 and $Z = 4$ [$R = 0.057$, $R_w = 0.054$ for 1882 independent reflections with $I > 3.0\sigma(I)$]; **4a**·CH_2Cl_2 triclinic $P\bar{1}$, with $a = 15.044(7)$, $b = 17.664(3)$, $c = 10.586(2)$ Å, $\alpha = 99.64(2)$, $\beta = 95.85(2)$, $\gamma = 94.74(2)°$, $V = 2744(1)$ Å^3, $Z = 2$ [$R = 0.065$, $R_w = 0.072$ for 4301 independent reflections $I > 3.0\sigma(I)$]; **5b** monoclinic, space group $P2_1/n$, $a = 15.036(4)$, $b = 17.192(5)$, $c = 15.983(3)$ Å, $\beta = 92.92(2)°$, $V = 4126(1)$ Å^3, $Z = 4$ [$R = 0.070$, $R_w = 0.079$ for 3389 independent reflections $I > 3\sigma(I)$]. Conformation of the ferrocenyl skeletons were determined by dihedral angles containing two Cp rings. In cyclic voltammertry (CV) of these complexes the Fe(II)/Fe(III) redox couples were quasi-reversible, but the Ru moieties were irreversible.

Keywords: (η6-Arene)ruthenium; Dppf–Ru complexes; Dpmf–Ru complexes; Electrochemistry

1. Introduction

1,1′-Bis(diphenylphosphino)ferrocene (dppf) is a well-known metalloligand and its chemistry has been well provided because of the conformational properties and the ligand of metal complex catalysts [1]. Since 1,1′-bis[-(diphenylphosphino)methyl]ferrocene (dpmf) formed by introduction of a methylene group between the cyclopentadienyl (Cp) ring and phosphorus atom could be more flexible than dppf, it is considered to have the possibility of various conformers between two Cp rings, as well as dppf. Our interest started from comparison of coordination modes between dpmf and dppf. We have reported that new dpmf was prepared from the reaction of 1,1′-bis(dichloromethyl)ferrocene with lithium diphenylphosphide and its molecule has a centrosymmetrical structure at an iron atom as well as that of dppf [2]. The reaction of dpmf with [$PdCl_2(MeCN)_2$] or $NiCl_2 \cdot 2H_2O$ gave a stable dimeric complex

* Corresponding author. Fax: + 81 474 751855.

[1] On leave from Changchun Institute of Applied Chemistry, Chinese Academy of Sciences.

0022-328X/98/$19.00
PII S0022-328X(98)00499-9

Table 1
Crystal data of (η^6-1,2,3,4-$Me_4C_6H_2$)$_2Ru_2C_4$(dpmf) **2a**, (η^6-1,2,3,5-$Me_4C_6H_2$)$_2Ru_2Cl_4$(dpmf)·$2CH_2Cl_2$ **2d**·$2CH_2Cl_2$, (η^6-1,2,3,4-$Me_4C_6H_2$)$_2Ru_2Cl_4$-(dppf)·CH_2Cl_2 **4a**, and [(η^6-Me_6C_6)RuCl(dppf)](PF_6) **5b**

Compound	**2a**	**2d**·$2CH_2Cl_2$	**4a**·CH_2Cl_2	**5b**
Formula	$C_{56}H_{60}Cl_4P_2FeRu_2$	$C_{58}H_{64}Cl_8P_2FeRu_2$	$C_{55}H_{58}Cl_6P_2FeRu_2$	$C_{46}H_{46}ClF_6P_3FeRu$
Molecular weight	1194.84	1364.70	1251.72	998.15
Color	Orange	Orange	Orange	Orange
Crystal dimensions (mm)	$0.20\times0.20\times0.20$	$0.30\times0.40\times0.1$	$0.50\times0.2\times0.10$	$0.40\times0.35\times0.12$
Scan rate, (° min^{-1})	16	2	8	4
Crystal system	Triclinic	Monoclinic	Triclinic	Monoclinic
Space group	$P1$ (no. 2)	$C2/c$ (no. 15)	$P1$ (no. 2)	$P2_1/n$ (no. 14)
Lattice parameters				
a	12.802(6)	38.379(6)	15.044(7)	15.036(4)
b	19.111(6)	9.903(3)	17.664(3)	17.192(5)
c	11.438(4)	17.381(4)	10.586(2)	15.983(3)
α	98.93(3)	90.0	99.64(2)	90.0
β	108.57(3)	113.91(1)	95.85(2)	92.92(2)
γ	90.42(3)	90.0	94.74(2)	90.0
V (Å^3)	2615(1)	6038(2)	2744(1)	4126(1)
Z	2	4	2	4
$D_{calc.}$ (g cm^{-3})	1.517	1.501	1.515	1.607
μ (cm^{-1})	11.45	11.73	11.89	9.60
$F(000)$	1216	2768	1268	2032
No. reflections	9219	5658	9660	7524
No. of data [$I>3.0\sigma(I)$]	4114	1882	4301	3389
No. of variables	586	307	590	523
R, R_w[a]	0.051, 0.052	0.057, 0.054	0.06, 0.072	0.070, 0.079
GOF[b]	1.39	1.48	1.98	2.30

[a] $R=\Sigma\|\|F_o|-|F_c\|/\Sigma|F_o|$ and $R_w=[\Sigma(|F_o|-|F_c|)^2/\Sigma w|F_o|^2]^{0.5}$ [$w=1/\sigma^2(F_o)$]
[b] GOF $=[\Sigma w(|F_o|-|F_c|)^2/\Sigma(N_o-N_v)]^{0.5}$, where N_o = number of data and N_v = number of variables.

$[M_2Cl_4(dpmf)_2]$ (M = Ni or Pd) which has a macrocyclic structure [2].

Arene ruthenium complexes played an important role as the precursors of catalysts in various organic syntheses [3]. Their research is one of very attractive subjects in the coordination chemistry. We reported previously that the reaction of $[(\eta^6\text{-arene})RuCl_2]_2$ with bulky and high basic aromatic phosphines bearing methoxy groups at 2- and 6-positions gave the complexes containing various coordination modes such as monohapto-(*P*-), dihapto- *(P,O-; P,OMe-)*, and trihapto-(*P,OMe,OMe; P,O,OMe; P,O,O*) [4]. We have interest in the reactions of bis[dichloro(η^6-arene)ruthenium(II)] with new flexible dpmf, particularly in confomations of ferrocenyl skeleton in metal complexes. For comparison, the reactions with dppf was also examined. A part of results has already been reported elsewhere [5].

2. Experimental

All reactions were carried out under nitrogen atmosphere. Bis[dichloro(η^6-arene)ruthenium(II)] [6], dpmf [2] and dppf [7] were prepared according to the literature. Dichloromethane, diethyl ether, and acetone were distilled over CaH_2. The IR spectra were measured on FT/IR-5300. NMR spectroscopy was carried out on a Bruker AC250. ^{1}H-NMR spectra were measured at 250 MHz using tetramethylsilane as an internal reference and $^{31}P\{^1H\}$-NMR spectra were measured at 101 MHz using 85% H_3PO_4 as an external reference. Electrochemical measurements were carried out in a 0.05 M solution of [*n*-Bu_4N][ClO_4]/MeCN–CH_2Cl_2 (1:1 ratio) under an atmosphere of nitrogen after the solution was deaerated by bubbling with nitrogen by use of a FUSO HECS3 17S Potentiostat Coulometer Timer and a FUSO HECS326 Digital Universal Signal Processing Unit. The measurements were a conventional three-electrode system: a Pt chip as a working electrode, a Pt wire as a counter electrode and an Ag|$AgNO_3$ (0.1 M)–[*n*-Bu_4N][ClO_4]/MeCN (0.1 M) reference electrode. All potentials are relative to a ferrocene/ferrocennium couple (1×10^{-3} M), whose potential was 145 mV versus a reference electrode.

*2.1. Reactions of [(η^6-arene)$RuCl_2$]$_2$ **1** with dppf and dpmf*

*2.1.1. Reaction of [(η^6-1,2,3,4-$Me_4C_6H_2$)$RuCl_2$]$_2$ **1a** with dpmf*

To a solution of **1a** (31 mg, 0.05 mmol) in CH_2Cl_2 (15 ml) was added dpmf (29 mg, 0.05 mmol) at room temperature (r.t.). After the mixture was stirred for 2 h,

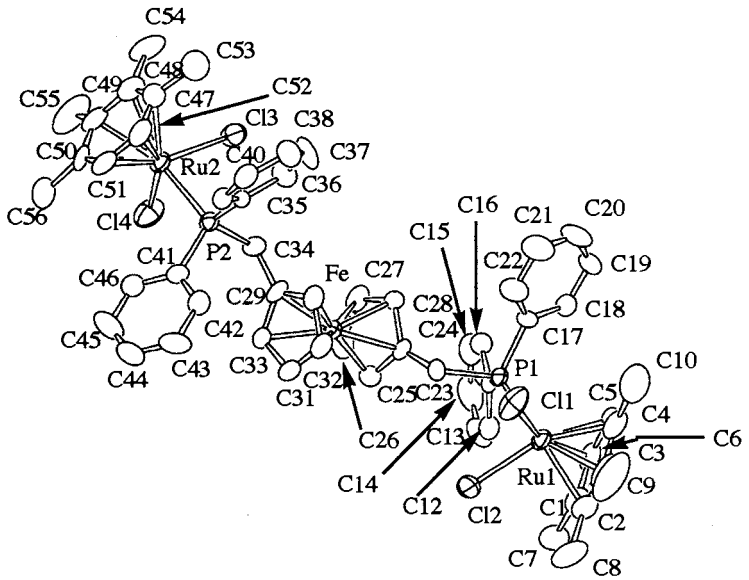

Fig. 1. Crystal structure of $[(\eta^6\text{-}1,2,3,4\text{-}Me_4C_6H_2)_2Ru_2C_4(dpmf)]$ **2a**. Hydrogen atoms are omitted for clarity.

the solvent was removed to ca. 3 ml under reduced pressure and ether was added to the solution to give orange crystals of $[(\eta^6\text{-}1,2,3,4\text{-}Me_4H_2C_6)RuCl_2]_2(\mu\text{-}$dpmf-*P*,*P*′) **2a**·$CH_2Cl_2$ (46 mg, 72%). ^{1}H-NMR ($CDCl_3$): δ 1.58 (s, C_6Me_2), 2.04 (d, $J_{PH} = 2.0$ Hz, C_6Me_2), 3.19 (s, CH_2), 3.46–3.56 (m, C_5H_4), 4.16 (d, $J_{PH} = 3.2$ Hz, $C_6Me_4H_2$), 5.30 (s, CH_2Cl_2), 7.2–7.7 (m, *Ph*) ppm. $^{31}P\{^1H\}$-NMR ($CDCl_3$): δ 32.41 (s) ppm. Anal. Calc. for $C_{57}H_{62}Cl_6P_2FeRu_2$: C 53.50, H 4.88. Found: C 53.86, H 4.79%.

2b (67%). ^{1}H-NMR ($CDCl_3$): δ 1.64 (s, C_6Me_6), 3.07 (s, CH_2), 3.42–3.51 (m, C_5H_4), 7.2–7.7 (m, *Ph*) ppm. $^{31}P\{^1H\}$-NMR ($CDCl_3$): δ 30.60 (s) ppm. Anal. Calc. for $C_{60}H_{68}Cl_4P_2FeRu_2$: C 57.61, H 5.48. Found: C 57.10, H 5.33%.

2c·$0.5CH_2Cl_2$ (59%). ^{1}H-NMR ($CDCl_3$): δ 0.82 (d, $J_{HH} = 6.7$ Hz, $CHMe_2$), 1.78 (s, *Me*), 2.49 (sep, $J_{HH} = 6.7$ Hz, CMe_2H), 3.12 (s, CH_2), 3.42–3.55 (m, C_5H_4), 5.12 (q, a center value of a A_2B_2 type, $J_{HH} = 5.7$ Hz, C_6H_4), 5.30 (s, CH_2Cl2), 7.3–7.7 (m, *Ph*) ppm. $^{31}P\{^1H\}$-NMR ($CDCl_3$): δ 28.14 (s) ppm. Anal. Calc. for $C_{56.5}H_{61}Cl_5P_2FeRu_2$: C 54.85, H 4.97. Found: C 54.83, H 4.69%.

2d·$1.5CH_2Cl_2$ (60%). ^{1}H-NMR ($CDCl_3$): δ 1.47 (s, C_6Me), 1.79 (s, C_6Me_2), 1.90 (s, C_6Me), 3.14 (s, CH_2), 3.44–3.55 (m, C_5H_4), 4.37 (s, C_6H_2), 5.30 (s, CH_2Cl_2), 7.2–7.7 (m, *Ph*) ppm. $^{31}P\{^1H\}$-NMR ($CDCl_3$): δ 30.79 (s) ppm. Anal. Calc. for $C_{57.5}H_{63}Cl_7P_2FeRu_2$: C 52.23, H 4.80. Found: C 52.20, H 4.66%.

2e·$0.5CH_2Cl_2$ (62%). ^{1}H-NMR ($CDCl_3$): δ 1.81 (d, $J_{PH} = 2.8$ Hz, C_6Me), 3.14 (s, CH_2), 3.44–3.58 (m, C_5H_4), 4.61 (s, C_6H_3), 5.30 (s, CH_2Cl_2), 7.2–7.7 (m, *Ph*) ppm. $^{31}P\{^1H\}$-NMR ($CDCl_3$): δ 29.84 (s) ppm. Anal. Calc. for $C_{54.5}H_{57}Cl_5P_2FeRu_2$: C 54.13, H 4.75. Found: C 53.54, H 4.70%.

2f (43%). ^{1}H-NMR ($CDCl_3$): δ 1.86 (s, C_6Me_2), 2.06 (s, C_6Me), 3.29 (s, CH_2), 3.51–3.62 (m, C_5H_4), 4.29 (d, $J_{HH} = 6.0$ Hz, C_6H_2), 4.62 (m, C_6H), 7.2–7.6 (m, *Ph*) ppm. $^{31}P\{^1H\}$-NMR ($CDCl_3$): δ 32.54 (s) ppm. Anal. Calc. for $C_{54}H_{56}Cl_4P_2FeRu_2$: C 55.59, H 4.84. Found: C 54.70, H 4.53%.

*2.1.2. Reaction of **2a** with xylyl isocyanide in the presence of $NaPF_6$*

To a mixture of **2a** (40 mg, 0.034 mmol) and xylyl isocyanide (17.6 mg, 0.13 mmol) in CH_2Cl_2 (5 ml) and acetone (5 ml) was added $NaPF_6$ (84 mg, 0.5 mmol) at r.t. After stirring for 4 h, the solvents were removed under reduced pressure and the residue was extracted with CH_2Cl_2 (2 × 10 ml). The solvent was concentrated to ca. 3 ml and ether was added to give orange crystals of **3a** (19 mg, 40%). ^{1}H-NMR (CD_2Cl_2): δ 1.54 (s, C_6Me_2), 2.09 (d, $J_{PH} = 2.3$ Hz, C_6Me), 3.14 (b, C_5H_2 and C_6H_2), 3.58 (bs, C_5H_2), 4.20 (d, $J_{PH} = 3.4$ Hz, C_6H_2), 7.3–7.6 (m, *Ph*) ppm. $^{31}P\{^1H\}$-NMR (CD_2Cl_2): δ 35.80 (s), −142.33 (sep, $J_{PH} = 710$ Hz) ppm. Anal. Calc. for $C_{56}H_{60}Cl_2P_4F_{12}FeRu_2$: C 47.57, H 4.28. Found: C 48.47, H 4.17.

*2.1.3. Reaction of $[(\eta^6\text{-}1,2,3,4\text{-}Me_4C_6H_2)RuCl_2]_2$ **1a** with dppf*

To a solution of **1a** (31 mg, 0.05 mmol) in CH_2Cl_2 (15 ml) was added dppf (28 mg, 0.05 mmol) at r.t. After the mixture was stirred for 2 h, the solvent was removed to ca. 3 ml under reduced pressure and ether was added to the solution to give orange crystals of $[(\eta^6\text{-}1,2,3,4\text{-}Me_4C_6H_2)RuCl_2]_2(\mu\text{-dppf-}P,P')$]
4a·$0.5CH_2Cl_2$ (75%). ^{1}H-NMR ($CDCl_3$): δ 1.68 (s, C_6Me_2), 2.05 (d, $J_{PH} = 2.5$ Hz, C_6Me_2), 3.9–4.1 (m, C_5H_4 and C_6H_2), 7.2–7.7 (m, *Ph*) ppm. $^{31}P\{^1H\}$-NMR

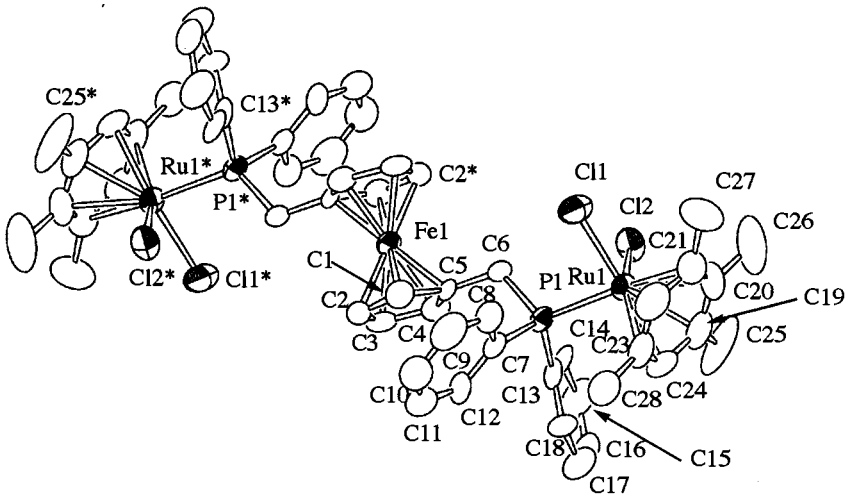

Fig. 2. Crystal structure of (η^6-1,2,3,5-$Me_4C_6H_2$)$_2Ru_2Cl_4$(dpmf)·$2CH_2Cl_2$ **2d**·$2CH_2Cl_2$. Hydrogen atoms, solvated molecules and PF_6 are omitted for clarity.

($CDCl_3$): δ 20.70 (s) ppm. Anal. Calc. for $C_{54.5}H_{57}Cl_5P_2FeRu_2$: C 54.13, H 4.75. Found: C 54.33, H 4.69%.

4b·$0.5CH_2Cl_2$ (65%). ^{1}H-NMR ($CDCl_3$): δ 1.58 (s, C_6Me_6), ca. 4.0 (b, C_5H_4), 5.30 (s, CH_2Cl_2), 7.2–7.6 (m, *Ph*) ppm. $^{31}P\{^1H\}$-NMR ($CDCl_3$): δ 20.16 (bs) ppm. Anal. Calc. for $C_{58.5}H_{65}Cl_5P_2FeRu_2$: C 55.53, H 5.18. Found: C 55.77, H 5.14%.

4c·$1.5CH_2Cl_2$ (69%). ^{1}H-NMR ($CDCl_3$): δ 0.96 (d, $J_{HH} = 6.9$ Hz, $CHMe_2$), 1.72 (s, C_6Me), 2.51 (sep, $J_{HH} = 6.9$ Hz, $CHMe_2$), 3.87 (s, C_5H_2), 4.16 (s, C_5H_2), 5.07 (m, C_6H_4), 5.30 (s, CH_2Cl_2), 7.3–7.8 (m, *Ph*) ppm. $^{31}P\{^1H\}$-NMR ($CDCl_3$): δ 18.50 (s) ppm. Anal. Calc. for $C_{55.5}H_{59}Cl_7P_2FeRu_2$: C 51.51, H 4.59. Found: C 51.61, H 4.56%.

4d·$2CH_2Cl_2$ (46%). ^{1}H-NMR ($CDCl_3$): δ 1.55 (s, C_6Me), 1.86 (s, C_6Me_2), 1.95 (s, C_6Me), ca. 4.0 (b, C_6H_2 and C_5H_2), 5.30 (s, CH_2Cl_2), 7.2–7.7 (m, *Ph*) ppm. $^{31}P\{^1H\}$-NMR ($CDCl_3$): δ 21.00 (s) ppm. Anal. Calc. for $C_{56}H_{60}Cl_8P_2FeRu_2$: C 50.32, H 4.52. Found: C 50.89, H 4.51%.

4e·$0.5CH_2Cl_2$ (63%). ^{1}H-NMR ($CDCl_3$): δ 1.85 (s, $C_6H_3Me_3$), ca. 4.0 (m, C_5H_4), 4.37 (s, C_6H_3), 5.30 (s, CH_2Cl_2), 7.3–7.7 (m, *Ph*) ppm. $^{31}P\{^1H\}$-NMR ($CDCl_3$): δ 20.24 (s) ppm. Anal. Calc. for $C_{52.5}H_{53}Cl_5P_2FeRu_2$: C 53.38, H 4.52. Found: C 52.95, H 4.42%.

4f·$0.5CH_2Cl_2$ (49%). ^{1}H-NMR ($CDCl_3$): δ 1.87 (s, C_6Me_2), 2.04 (s, C_6Me), 3.90–4.04 (m, C_5H_4 and C_6H_2), 5.30 (s, CH_2Cl_2), 4.65 (m, C_6H), 7.2–7.6 (m, *Ph*) ppm. $^{31}P\{^1H\}$-NMR ($CDCl_3$): δ 20.54 (s) ppm. Anal. Calc. for $C_{52.5}H_{53}Cl_5P_2FeRu_2$: C 53.38, H 4.52. Found: C 53.90, H 4.51%.

2.1.4. Reaction of [(η^6-1,2,3,4-$Me_4C_6H_2$)$RuCl_2$]$_2$ 1a with dppf in the presence of $NaPF_6$

To a mixture of **1a** (31 mg, 0.05 mmol) and dppf (55 mg, 0.10 mmol) in CH_2Cl_2 (15 ml) and acetone (10 ml) was added $NaPF_6$ (84 mg, 0.5 mmol) at r.t. After the mixture was stirred for 2 h, the solvent was removed under reduced pressure and the residue was extracted with CH_2Cl_2. The solvent was concentrated to 3 ml, and ether was added to the solution to give orange crystals of [(η^6-1,2,3,4-$Me_4H_2C_6$)RuCl(dppf-*P*,*P*′)](PF_6) **5a** (25 mg, 26%). IR (nujol): 833 cm^{-1} (PF_6). ^{1}H-NMR ($CDCl_3$): δ 1.28 (bs, C_6Me_2), 1.92 (bs, C_6Me_2), 4.01, 4.19, 4.30, 5.04 (s, C_5H), 4.84 (bs, C_6H_2), 7.3–7.7 (m, *Ph*) ppm. $^{31}P\{^1H\}$-NMR ($CDCl_3$): 636.67 (s), −144.5 (sep, $J_{PF} = 710$ Hz) ppm. Anal. Calc. for $C_{44}H_{42}ClF_6P_3FeRu$: C 54.48, H 4.36. Found: C 54.13, H 4.21%.

5b (76%). IR (nujol): 839 cm^{-1} (PF_6). ^{1}H-NMR ($CDCl_3$): δ 1.53 (s, C_6Me_6), 3.98, 4.11, 4.25, 4.94 (s, C_5H), 7.47.9 (m, *Ph*) ppm. $^{31}P\{^1H\}$-NMR ($CDCl_3$): δ 33.96 (s), −144.6 (sep, $J_{PF} = 710$ Hz) ppm. Anal. Calc. for $C_{46}H_{46}ClF_6P_3FeRu$: C 55.35, H 4.62. Found: C 55.40, H 4.38%.

5c (56%). IR (nujol): 839 cm^{-1} (PF_6). ^{1}H-NMR ($CDCl_3$): δ 0.85 (d, $J_{HH} = 7.0$ Hz, $CHMe_2$), 0.94 (s, C_6Me), 2.65 (sep, $J_{HH} = 7.0$ Hz, $CHMe_2$), 4.05, 4.25, 4.33, 5.04 (s, C_5H), 5.10 (d, $J_{HH} = 5.0$ Hz), 5.68 (c, C_6H_2), 7.4–7.7 (m, *Ph*) ppm. $^{31}P\{^1H\}$-NMR ($CDCl_3$): δ 36.52 (s), −144.3 (sep, $J_{PF} = 710$ Hz) ppm. Anal. Calc. for $C_{44}H_{42}ClF_6P_3FeRu$: C 54.48, H 4.36. Found: C 54.16, H 4.28%.

5d (52%). IR (nujol): 833 cm^{-1} (PF_6). ^{1}H-NMR ($CDCl_3$): δ 1.36 (bs, C_6Me), 1.59 (bs, C_6Me_2), 3.89, 3.95, 4.32, 5.17 (s, C_5H), 4.98 (bs, C_6H_2), 7.47.7 (m, *Ph*) ppm. $^{31}P\{^1H\}$-NMR ($CDCl_3$): δ 34.61 (s), −144.4 (sep, $J_{PF} = 710$ Hz) ppm. Anal. Calc. for $C_{44}H_{42}ClF_6P_3FeRu$: C 54.48, H 4.36. Found: C 53.76, H 4.09%.

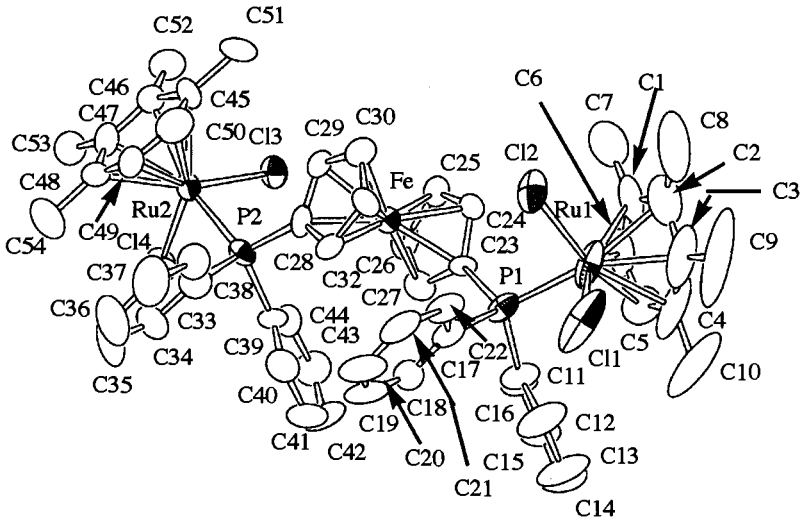

Fig. 3. Crystal structure of (η^6-1,2,3,4-$Me_4C_6H_2$)$_2Ru_2Cl_4$(dppf)·CH_2Cl_2 **4a**. Hydrogen atoms and CH_2Cl_2 are omitted for clarity.

5e (67%). IR (nujol): 837 cm^{-1} (PF_6). ^{1}H-NMR ($CDCl_3$): δ 1.73 (s, $C_6H_3Me_3$), 3.98, 4.08, 4.30, 5.08 (s, C_5H), 4.83 (s, C_6H_3), 7.47.9 (m, *Ph*) ppm. $^{31}P\{^1H\}$-NMR ($CDCl_3$): δ 35.17 (s), −144.3 (sep, $J_{PF} = 710$ Hz) ppm. Anal. Calc. for $C_{43}H_{40}ClF_6P_3FeRu$: C 54.02, H 4.22. Found: C 54.07, H 4.27%.

5f (31%). IR (nujol): 839 cm^{-1} (PF_6). ^{1}H-NMR ($CDCl_3$): δ 1.57 (bs, C_6Me_2), 1.88 (bs, C_6Me), 4.05, 4.26, 4.35, 5.18 (s, C_5H), 4.66 (bs, C_6H_2), 5.45 (bs, C_6H), 7.47.8 (m, *Ph*) ppm. $^{31}P\{^1H\}$-NMR ($CDCl_3$): δ 36.53 (s), −144.3 (sep, $J_{PF} = 710$ Hz) ppm. Anal. Calc. for $C_{43}H_{40}ClF_6P_3FeRu$: C 54.02, H 4.22. Found: C 53.38, H 3.95%.

2.1.5. Reaction of [(η^6-C_6Me_6)RuCl{P(2-o-6-$MeOC_6H_3Ph_2$}] with dpmf in the presence of $NaPF_6$

To a mixture of [(η^6-C_6Me_6)RuCl{P(2-*o*-6-$MeOC_6H_3$)Ph_2}] (59 mg, 0.10 mmol) and dpmf (29 mg, 0.05 mmol) in CH_2Cl_2 (15 ml) and acetone (10 ml) was added Na_4PF_6 (33 mg, 0.20 mmol) at r.t. After the mixture was stirred for 2 h, the solvent was removed under reduced pressure and the residue was extracted with CH_2Cl_2. The solvent was concentrated to 3 ml, and ether was added to the solution to give orange crystals of [(η^6-C_6Me_6)Ru{P(2-*o*-6-$MeOC_6H_3Ph_2$}]$_2$(dpmf) **6** (25 mg, 25.3%). IR (nujol): 1578, 1551, 835 cm^{-1} (PF_6). $^{31}P\{^1H\}$-NMR (CD_2Cl_2): A; δ 31.45 (d, $J_{PP} = 50.1$ Hz, dpmf), 50.84 (d, $J_{PP} = 50.1$ Hz, MDMPP-O,*P*); B; 31.14 (d, $J_{PP} = 50.1$ Hz, dpmf), 50.90 (d, $J_{PP} = 50.1$ Hz, MDMPP-O,*P*); −142.4 (sep, $J_{PF} = 706.0$ Hz) ppm. Anal. Calc. for $C_{98}H_{100}O_4F_{12}P_6FeRu_2$: C 58.45, H 5.01. Found: C 58.41, H 5.03%.

2.2. X-ray analysis

2.2.1. Data collection

Complexes **(2a, 2d**·$2CH_2Cl_2$, **4a**·CH_2Cl_2 and **5b)** were recrystallized from CH_2Cl_2/ether. Cell constants were determined from 15–20 reflections on Rigaku four-circle automated diffractometer AFC5S. The crystal parameters along with data collections are summarized in Table 1. Data collection was carried out by a Rigaku AFC5S diffractometer. Intensities were measured by the $2\theta - \omega$ scan method using Mo–K_α radiation ($\lambda = 0.71069$ Å). Throughout the data collection the intensities of the three standard reflections were measured every 200 reflections as a check of the stability of the crystals and any decay was not observed. Intensities were corrected for Lorentz and polarization effects. The absorption correction was made. Atomic scattering factors were taken from the usual tabulation [8]. Anomalous dispersion effects were included in F_{calc} [9]; the values of $\Delta f'$ and $\Delta f''$ were from Creagh and McAuley [10]. All calculations were performed using the teXsan crystallographic software package of Molecular Structure Corporation.

2.2.2. Determination of the structures

The structure of **2a** was solved by direct methods and **2d**·$2CH_2Cl_2$, **4a**·CH_2Cl_2 and **5b** were solved by Patterson methods (DIRDIF92 PATTY). The ruthenium and iron atoms were located in the initial E map, and subsequent Fourier syntheses gave the positions of other non-H atoms. The iron atom of **2d**·$2CH_2Cl_2$ was occupied at the center of the symmetry. Hydrogen atoms were calculated at the ideal

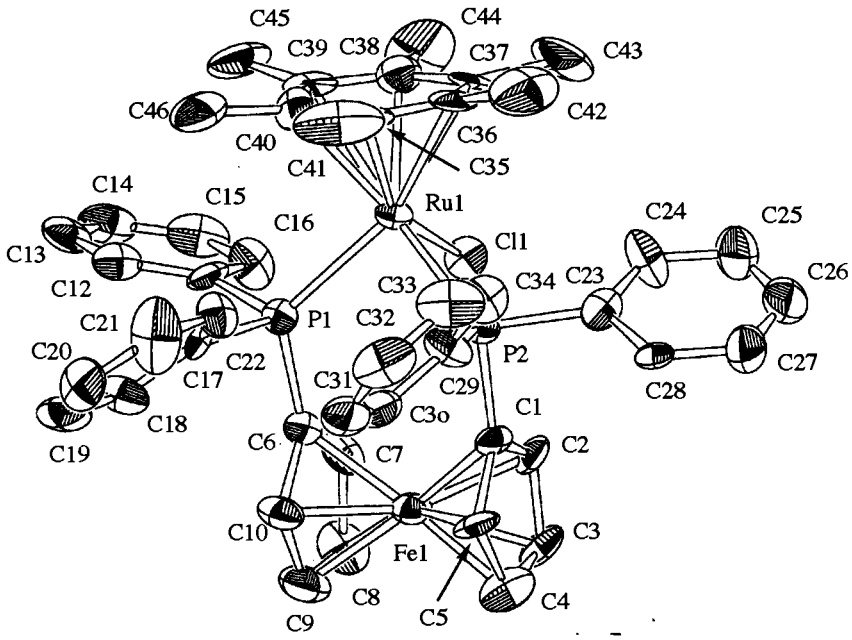

Fig. 4. Crystal structure of $[(\eta^6\text{-}Me_6C_6)RuCl(dppf)](PF_6)$ **5b**. Hydrogen atoms and PF_6 are omitted for clarity.

positions with the C–H distance of 0.95 Å, and were not refined. The positions of the non-H atoms were refined with anisotropic thermal parameters by using full-matrix least-squares methods. Final difference Fourier syntheses showed peaks at heights up to 0.88–1.10 e $Å^{-3}$.

3. Results and discussion

3.1. Reactions of $[(\eta^6\text{-arene})_2Ru_2Cl_4]$ 1 with dpmf

When arene ruthenium complexes $[(\eta^6\text{-arene})_2Ru_2Cl_4]$ **1** (arene = (**a**) 1,2,3,4-$Me_4C_6H_2$; (**b**) C_6Me_6; (**c**) *p*-cymene; (**d**) 1,2,3,5-$Me_4C_6H_2$; (**e**) 1,3,5-$Me_3C_6H_3$; (**f**) 1,2,3-$Me_3C_6H_3$) were treated with dpmf in CH_2Cl_2 at r.t. in a 1:1 ratio, orange or reddish orange crystals **2**, formulated as $[(\eta^6\text{-arene})_2Ru_2Cl_4(dpmf)]$, were isolated. The structures of these complexes were confirmed by X-ray analyses of **2a** and **2d**. Molecules displayed a three-legged piano-stool structure which the (arene)ruthenium moiety was surrounded by a phosphorus and two chloride atoms, and two arene ruthenium moieties were bridged through the dpmf ligand (Figs. 1 and 2) (vide infra).

In the ^{1}H-NMR spectrum in $CDCl_3$ one of two kinds of methyl protons of **2a** and the methyl protons of **2e** appeared at δ 2.04 and 1.81 ppm as a doublet by coupling with the phosphorus nuclei, respectively, whereas in other complexes they appeared as a singlet without showing coupling. The α- and β-protons of the Cp rings were observed as singlets in the range of δ 3.1–3.6 ppm, shifting to the higher field by ca. 0.4–0.7 ppm than those of free dpmf.

In the $^{31}P\{^1H\}$-NMR spectra the chemical shift of the coordinated dpmf ligand appeared as a singlet at δ ca. 30 ppm, shifting to the down field compared with that of free dpmf, in which the chemical shift difference ($\Delta = \delta_{com} - \delta_{free}$) between free and coordinated dpmf's is ca. 42 ppm. There is no systematic relationship between the number of the methyl groups and chemical shifts, but in the complexes bearing the same number of methyl groups (for example: **2a** and **2d**, and **2e** and **2f**), the chemical shifts of the complexes containing the high

Table 2
Selected bond lengths (Å), angles (°) and torsion angles (°) of 2a

Bond lengths (Å)			
Ru(1)–Cl(1)	2.404(3)	Ru(1)–Cl(2)	2.406(3)
Ru(1)–P(1)	2.340(3)	Ru(2)–Cl(3)	2.407(3)
Ru(2)–Cl(4)	2.407(3)	Ru(2)–P(2)	2.349(3)
Ru–C(arene)	2.21[a]	Fe–C(Cp)	2.04[a]
Bond angles (°)			
Cl(1)–Ru(1)–Cl(2)	88.3(1)	Cl(1)–Ru(1)–P(1)	82.8(1)
Cl(2)–Ru(1)–P(1)	88.1(1)	Cl(3)–Ru(2)–Cl(4)	88.3(1)
Cl(3)–Ru(2)–P(2)	84.20(10)	Cl(4)–Ru(2)–P(2)	87.6(1)
Ru(1)–P(1)–C(11)	105.2(5)	Ru(1)–P(1)–C(17)	113.3(3)
Ru(1)–P(1)–C(23)	113.8(3)	C(11)–P(1)–C(17)	105.2(5)
C(11)–P(1)–C(23)	105.4(4)	C(17)–P(1)–C(23)	105.4(4)
Ru(2)–P(2)–C(34)	114.5(3)	Ru(1)–P(2)–C(35)	109.9(3)
Ru(2)–P(2)–C(41)	116.1(3)	C(34)–P(2)–C(35)	106.8(5)
C(34)–P(2)–C(41)	104.7(4)	C(35)–P(2)–C(41)	103.9(5)
C(24)–Fe–C(29)	158.3(4)		
Torsion angles (°)			
Ru(1)–P(1)–C(23)–C(24)	−151.0(6)	Ru(2)–P(2)–C(34)–C(29)	−166.1(7)

[a] Mean values between metal (Ru or Fe) and carbon atoms of the arene or Cp ring.

Table 3
Selected bond lengths (Å) and angles (°) of $2d \cdot 2CH_2Cl_2$

Bond lengths (Å)			
Ru(1)–Cl(1)	2.402(4)	Ru(1)–Cl(2)	2.403(3)
Ru(1)–P(1)	2.342(3)		
Ru–C(arene)	2.21[a]	Fe–C(Cp)	2.04[a]
Bond angles (°)			
Cl(1)–Ru(1)–Cl(2)	87.8(1)	Cl(1)–Ru(1)–P(1)	87.4(1)
Cl(2)–Ru(1)–P(1)	84.4(1)		
Ru(1)–P(1)–C(6)	115.9(4)	Ru(1)–P(1)–C(7)	117.3(4)
Ru(1)–P(1)–C(13)	105.7(5)	C(6)–P(1)–C(7)	100.8(5)
C(6)–P(1)–C(13)	105.7(5)	C(7)–P(1)–C(13)	105.6(6)
C(5)–Fe–C(5)[a]	180.0		
Torsion angle (°)			
Ru(1)–P1–C6–C5	−179.7(8)		

[a] Mean values between metal (Ru or Fe) and carbon atoms of the arene or Cp ring.

symmetrical arene rings appeared at the upper field. The electron richness of arene ligand is not the only factor which contributes to the chemical shift [11].

In some attempts to extract Cl anions the reactions of **2a** with PhC≡CH in alcoholic NaOH to prepare an alkynyl complex or with CO in the presence of $NaPF_6$ were undertaken, but no complexes identified were obtained. When **2a** was treated with xylyl isocyanide in the presence of $NaPF_6$ in a mixture of CH_2Cl_2 and acetone, unstable orange solids **3a** were isolated in 40% yield. Surprisingly an isocyanide molecule could not be confirmed from the IR spectrum, but it showed the presence of the PF_6 ligand at 841 cm^{-1}. Complex **3a** was formulated as $(1,2,3,4\text{-}Me_4C_6H_2)_2Ru_2Cl_2(dpmf)(PF_6)_2$ from an elemental analysis. The ^{1}H-NMR spectrum in CD_2Cl_2 showed five signals at δ 1.54 (s), 2.09 (d), 3.14 (br), 3.58 (br), 4.20 (d) ppm consisting of a 12:12:8:4:4 intensity ratio, in addition to at δ 7.3–7.6 ppm due to the aromatic protons, assigned as C_6Me_2, C_6Me_2, a sum of CH_2 and C_5H_2, C_5H_2, and aromatic protons of the arene, respectively. The NMR pattern was in close agreement with that of **2a**. The $^{31}P\{^1H\}$-NMR spectrum showed a singlet at 35.80 ppm, similar to that of **2a**. Since complex **3a** has a coordinatively unsaturated structure with a 16-electron count, it is assumed at present that one F atom of the PF_6 anions participated with coordination to metals to satisfy an 18-electron count. The detailed structure is remained unknown. The F-coordination of the PF_6 anion has been noted in various complexes [12].

Table 4
Selected bond lengths (Å), angles (°) and torsion angles (°) of $4a \cdot CH_2Cl_2$

Bond lengths (Å)			
Ru(1)–Cl(1)	2.404(5)	Ru(1)–Cl(2)	2.400(3)
Ru(1)–P(1)	2.350(4)	Ru(2)–Cl(3)	2.414(3)
Ru(2)–Cl(4)	2.399(3)	Ru(2)–P(2)	2.351(4)
Ru–C(arene)	2.22[a]	Fe–C(Cp)	2.04[a]
Bond angles (°)			
Cl(1)–Ru(1)–Cl(2)	88.7(1)	Cl(1)–Ru(1)–P(1)	87.2(2)
Cl(2)–Ru(1)–P(1)	87.8(1)	C1(3)–Ru(2)–Cl(4)	89.3(1)
Cl(3)–Ru(2)–P(2)	87.8(1)	C1(4)–Ru(2)–P(2)	88.1(1)
Ru(1)–P(1)–C(11)	108.8(4)	Ru(1)–P(1)–C(17)	122.9(4)
Ru(1)–P(1)–C(23)	113.9(4)	C(11)–P(1)–C(17)	98.8(6)
C(11)–P(1)–C(23)	105.4(5)	C(17)–P(1)–C(23)	104.9(5)
Ru(2)–P(2)–C(28)	114.8(4)	Ru(1)–P(2)–C(33)	108.3(5)
Ru(2)–P(2)–C(39)	121.6(4)	C(28)–P(2)–C(33)	103.1(6)
C(28)–P(2)–C(39)	104.7(5)	C(33)–P(2)–C(39)	102.3(6)
C(23)–Fe–C(28)	148.0(5)		

[a] Mean values between metal (Ru or Fe) and carbon atoms of the arene or Cp ring.

3.2. Reactions of $[(\eta^6\text{-arene})_2Ru_2Cl_4]$ 1 with dppf

It has been known that the reaction of **1c** with dppf gave the dppf bridged complex $[(p\text{-cymene})RuCl_2]_2(\mu\text{-dppf-}P,P')$, but the detailed structural analysis has not yet been examined [13]. To compare reactivity between dpmf and dppf and to obtain detailed structural information, reactions of **1** with dppf were carried out. When **1** was treated with dppf in a 1:1 ratio in CH_2Cl_2 at r.t., orange crystals formulated as $[(\eta^6\text{-arene})RuCl_2]_2$(dppf) **4** and were obtained in 50–75% yields. The molecule was confirmed to have a structure similar to that of **2** by an X-ray analysis of $[(\eta^6\text{-}1,2,3,4\text{-}Me_4C_6H_2)RuCl_2]_2(\mu\text{-dppf-}P,P')$ **4a** (Fig. 3).

In the ^{1}H-NMR spectrum of **4a**, one of two kinds of methyl protons on the arene rings was observed as doublets and another one as a singlet, which was also the case in **2**. In other complexes they appeared as singlets.

The α- and β-protons of the Cp rings could be classified by two types of signals. In **4a**, **4c**, and **4f** they were observed as two singlets at δ ca 4.0 ppm, whereas in **4b**, **4d**, and **4e** they were observed as one broad signal. When the spectra of **4d** and **4e** were measured at 50°C, one broad signal was separated as two broad singlets at δ 4.04 and 4.15 ppm for **4e**, and at δ 4.03 and 4.11 ppm for **4d**, respectively, assignable to either of the α- or β-protons on the Cp rings, but that of **4b** was kept still broad, likely due to the more steric demand of hexamethybenzene than 1,3,5-trimethylbenzene and 1,2,3,5-tetramethylbenzene.

The difference in the NMR behaviour is assumed to be responsible for the methyl groups on the arene rings but this does not necessarily depend on the number of the substituent groups on the arene rings, as found between 1,2,3,5- and $1,2,3,4\text{-}Me_4C_6H_2$ complexes and between 1,3,5- and $1,2,3\text{-}Me_3C_6H_3$ complexes, but appears to depend on the partial crowding in the arene rings. Similar behavior has been noted for reactivities of (2,6-dimethoxyphenyl)diphenylphosphine toward bis[dichloro(η^6-arene)ruthenium(II)] [4]. The $^{31}P\{^1H\}$-NMR spectrum appeared at δ ca. 20 ppm, shifting to the down field by 37 (Δ) ppm compared with the chemical shift of free dppf and to the higher field by ca. 10 ppm than those

Table 5
Structural parameters of the ferrocenyl skeleton

	τ (°)[a]	θ (°)[b]	C_A–Fe–C_B (°)	P···P (Å)	Conformation
dpmf	180.0	0	180.0	9.61	Antiperiplanar
2a	141.0	1.4	158.3	9.35	Anticlinal (eclipsed)
2d	180.0	0	180.0	9.62	Antiperiplanar
4a	118.6	4.4	148.0	6.43	Anticlinal (staggered)
5b	3.9	4.5	105.4	3.41	Synperiplanar

[a] The torsion angle is defined as C_A–X_A–X_B–C_B, where C_A is carbon atom in Cp ring A that is bonded to a P atom or CH_2 group (likewise for C_B) and X_A and X_B are the centroids of the two Cp rings.
[b] θ is the dihedral angles between the two Cp rings.

of the corresponding bridged dpmf complexes, arising from higher nucleophilicity of dpmf compared with dppf.

An attempt to replace Cl anions by CO in the presence of $NaPF_6$ was unsuccessful to obtain isolable complexes.

3.3. Reactions of $[(\eta^6\text{-arene})_2Ru_2Cl_4]$ **1** with dppf in the presence of $NaPF_6$

When **1a** was treated with dppf in a 1:2 molar ratio in the presence of $NaPF_6$ at r.t., orange crystals **5a** formulated as $[(\eta^6\text{-}1,2,3,4\text{-}Me_4C_6H_2)RuCl(dppf)](PF_6)$ were obtained in 26% yield. Complexes bearing the arene rings such as C_6Me_6 (**5b**), *p*-cymene (**5c**), 1,2,3,5-$Me_4C_6H_2$ (**5d**), 1,3,5-$Me_3C_6H_3$ (**5e**), and 1,2,3-$Me_3C_6H_3$ (**5f**) could be readily prepared from the reactions of dppf with the corresponding arene ruthenium complexes in the presence of $NaPF_6$. The presence of the PF_6 group in **5** was confirmed by an appearance of a strong band at ca. 840 cm^{-1}.

The methyl and aromatic protons on the arene rings of **5b**, **5c** and **5e** appeared as sharp singlets without showing the coupling with coordinated phosphorus atoms. However those of **5a**, **5d** and **5f** bearing partially-crowded arene rings displayed broad singlets.

The characteristic feature is the presence of four kinds of protons in the range from δ 4.0 to 5.0 ppm responsible for the protons of Cp rings. For example, **5b** showed four singlets at 3.98, 4.11, 4.30, 5.05 and 5.04 ppm. This inequivalence is responsible for the rigid ferrocene moiety by the chelation of the dppf ligand, as depicted in Fig. 4.

The $^{31}P\{^1H\}$-NMR spectra appeared at δ ca. 35 ppm, being a downfield shift of ca. 15 ppm compared with those of the corresponding bridged dppf complexes, likely due to a salt-like complexes.

Similar reactions with dpmf were carried out to isolate the chelated dpmf complexes, but such complexes could not be obtained. An introduction of the CH_2 group between the Cp ring and P atom appear to prevent the chelation conformation, because of its high freedom and long P–P distance.

When dpmf was treated with $(\eta^6\text{-}C_6Me_6)RuCl$-(MDPMPP-*P*,*O*) [MDMPP-*P*,*O* = 2-*o*-6-$MeOC_6H_3$)-Ph_2P] in a 1:2 ratio in the presence of an excess of $NaPF_6$ at r.t., orange crystals **6** formulated as $[\{(\eta^6\text{-}C_6Me_6)Ru$-(MDMPP-*P*,*O*)$\}_2$(dpmf)$](PF_6)_2$ were obtained. The $^{31}P\{^1H\}$-NMR spectrum showed four doublets with two pairs of 31.45/50.84 (A) and 31.14/50.9 (B) ppm consisting of $J_{PP} = 50.1$ Hz, and the intensity ratio between A and B is 2:3. The signals at δ ca. 31 ppm are assignable to dpmf, and those at δ ca. 50 ppm to other P nuclei. This spectrum is a result of the diastereomers derived from two chiral Ru centers.

3.4. Molecular structures

3.4.1. Complexes **2a**, **2d**·$2CH_2Cl_2$, and **4a**·CH_2Cl_2

Complexes **2d** and **4a** were crystallized to contain CH_2Cl_2 as a solvated molecule. The molecules of **2a**, **2d**·CH_2Cl_2 and **4a**·CH_2Cl_2 consist of the dinuclear structures bridged by dpmf or dppf ligand. Complex **2d**·CH_2Cl_2 has a centrosymmetric structure with an inversion center at a Fe atom. The ruthenium atoms are surrounded by arene, P and two Cl atoms and the molecules have the three-legged piano-stool conformation. The selected bond lengths and angles are listed in Tables 2–4.

The Ru–Cl and Ru–P lengths of **2a**, **2d** and **4a** are ca. 2.40 and 2.34 Å, and the average values of the Ru–C and Fe–C lengths concerning the Ru–arene and Fe–Cp bonds are 2.20 and 2.04 Å, respectively. Their values do not depend on arene and phosphorus ligands.

In the dpmf complexes (**2a** and **2d**), the Cl–Ru–Cl angle and one of the P–Ru–Cl bond angles are ca. 88° and another P–Ru–Cl one is ca. 84°, whereas the Cl–Ru–Cl and P–Ru–Cl angles of the dppf complex **4a** are similar values with ca. 88°, likely minimizing steric repulsion due to higher rigidity of dppf than dpmf.

The structural parameters of the ferrocenyl skeleton are listed in Table 5. The dihedral angles between two Cp rings are 1.4° for **2a**, 0° for **2d** and 4.4° for **4a**, being not significantly different from those found in other dppf complexes.

The conformation of dppf in the dppf complexes has been classified by six categories which were defined by torsion angles (τ) C_A–X_A–X_B–C_B, where C_A is a carbon atom in Cp ring A that is bonded to a P atom

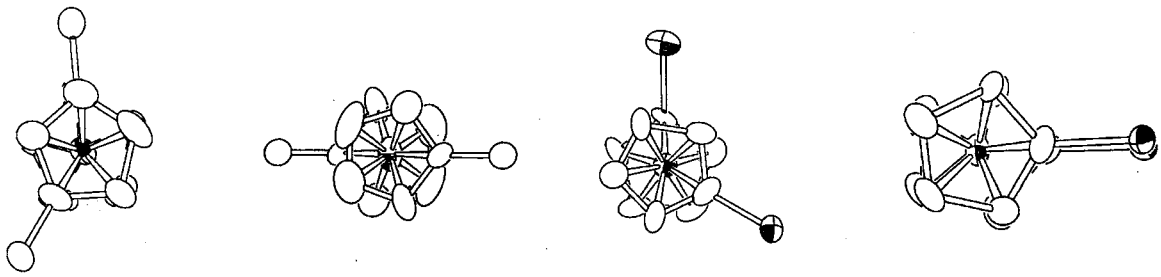

2a: anticlinal (eclipsed) **2d**: antiperiplanar **4a**: anticlinal (staggered) **5b**: synperiplanar

Fig. 5. Conformations of the ferrocenyl rings.

(likewise for C_B) and X_A and X_B are the centroids of the two Cp rings [1]. The classification could be also applied in dpmf complexes. The torsion angles of **2a**, **2d** and **4a** are 141.0, 180.0 and 118.6°, respectively. Their results suggested that conformations of the two Cp rings were anticlinal (eclipsed) for **2a**, antiperiplanar for **2d**, and anticlinal (staggered) for **4a**, respectively, as depicted in Fig. 5. Anticlinal (eclipsed) conformation has been observed in a three-legged piano-stool complex (η^5-MeCp)Mn(CO)$_2$(dppf-*P*) [14] and in octahedral complexes [$Mn_2(CO)_9$]$_2$(μ-dppf) [15], *cis*-[Mo(CO)$_5$(dppf-*P*)] [16], and [$Re_2(CO)_9$]$_2$(μ-dppf) [15]. Antiperiplanar ones have been noted in [M(CO)$_5$]2(μ-dppf) (M = Cr, Mo) [17] and *cis*-[$Mn_2Cl_2(CO)_8$(μ-dppf)] [18] in addition to free dppf [19] and dmpf [3]. There are known a few complexes having an anticlinal staggered conformation, and one of them is Ag_2(μ-$C_6H_5CO_2$)(μ-dppf) [20].

3.4.2. Complex **5b**

The Ru atom of **5b** is surrounded by an arene, one Cl atom, and two P atoms of the chelated dppf, showing a three-legged piano-stool structure (Fig. 4). Selected bond lengths and angles are listed in Table 6.

The Ru–Cl bond length of 2.396(3) Å is not significantly different from those of the μ-bridged complexes, but the Ru–P bond lengths of 2.362(3) and 2.377(3) Å are slightly longer than those in neutral complexes **2** and **4**, in spite of being a salt-like complex, because of the steric demand of bulky chelated dppf. The average Ru–C(arene) length of 2.34 Å is longer than those found in the bridged dppf and dpmf complexes, again due to steric demand of chelated dppf. The average Fe–Cp length is 2.03 Å, being not significantly different from those of the bridged complexes. The P–Ru–Cl angles are similar to those of the bridged complexes. The P–Ru–P bite angle of 92.0(1)° is similar to that (91.6°) of $C_5Me_5RuO_2$(dppf-*P*,*P*′) [21]. The dihedral angle of 45° between the two Cp rings is also similar to those of the bridged complexes. The torsion angle of 3.9° is equal to a synperiplanar conformation, which has been observed in square-planar and three-legged piano-stool complexes such as NiX_2(dppf-*P*,*P*′) (X = Cl [19]; X = Br [22]) and (η^5-MeCp)Mn(CO)(dppf-*P*,*P*′)·$CHCl_3$ [13,23].

An attempt to replace a Cl anion in the presence of xyly isocyanide by NH_4PF_6 recovered the starting materials quantitatively. Extraction of Cl anions from the ruthenium dppf or dpmf complexes appears to be more difficult than those in other phosphine complexes, likely resulting in steric demand.

3.5. Electrochemical reactions

The electrochemistry of compounds **2**, **4** and **5** was studied by cyclic voltammertry (CV), which was performed in CH_2Cl_2/MeCN (a 1:1 ratio) at r.t. with 0.1 M solution of [*n*-Bu_4N][ClO_4] as the supporting electrolyte, and all $E_{1/2}$ values are given versus the $F_c/[F_c]^+$ [F_c = (η^5-$C_5H_5)_2$Fe] redox couple (Table 7).

The CV showed one quasi-reversible and one irreversible waves in the positive region; the former is assigned to the Fe(II)/Fe(III) couple and the latter to oxidation of Ru(II) because such oxidation waves were not observed in dpmf or dppf. The Fe(II)/Fe(III) couples appeared at −40 mV for **2**, 170 mV for **4** and 40 mV for **5**, respectively. In the bridged complexes the Fe(II)/Fe(III) redox potentials were not significantly different from those found in each free ligand. The redox reactions of the dpmf complexes were performed much easily than those of dppf ones, reflecting the electrochemical behaviors of free ligands. The chelated complexes showed higher redox potentials in comparison with those of the neutral complexes, depending on electron-deficient property of **5** [2].

Table 6
Selected bond lengths (Å) and angles (°) for 5b

Bond lengths (Å)			
Ru(1)–Cl(1)	2.396(3)	Ru(1)–P(1)	2.362(3)
Ru(1)–P(2)	2.377(3)		
Ru–C(arene)	2.34[a]	Fe–C(Cp)	2.03[a]
Bond angles (°)			
Cl(1)–Ru(1)–P(1)	88.8(1)	Cl(1)–Ru(1)–P(2)	86.4(1)
P(1)–Ru(1)–P(2)	92.0(1)	Ru(1)–P(1)–C(6)	122.0(4)
Ru(1)–P(1)–C(17)	113.3(3)	Ru(1)–P(2)–C(1)	121.5(4)
C(1)–Fe–C(6)	105.4(5)		

[a] Mean values between metal (Ru or Fe) and carbon atoms of the arene or Cp ring.

Table 7
Electrochemical data for complexes **2**, **4** and **5**[a]

Complex	**2**		**4**		**5**	
	$E_{1/2}$(Fe)	E_{pa}(Ru)	$E_{1/2}$(Fe)	E_{pa}(Ru)	$E_{1/2}$(Fe)	E_{pa}(Ru)
a	−35	[b]	170	[b]	393	[b]
b	−60	750	111	533	373	1300
c	[b]	875	168	733	420	1420
d	−40	875	168	650	393	[b]
e	−32	785	185	680	388	1405
f	−20	[b]	195	690	414	[b]

[a] Measured in a 0.1 M [n-Bu_4N][ClO_4]/MeCN–CH_2Cl_2 (1:1). Scan time: 0.10 V s^{-1} for **2** and **5**, and 0.05 V s^{-1} for **4**. $E_{1/2}$ and E_{pa} values are given versus ferrocene/ferrocenium couple ($E \pm 10$ mV).
[b] Clear peak was not observed.

In general, increased electron-donating ability of the arenes affects the $E_{1/2}$ values of redox potentials [24]. In [(η^6-arene)Ru(dppe)]$^{2+}$ a linear fashion has been observed between the $E_{1/2}$ values for the Ru(II)/Ru(III) couples and the number of methyl groups. The $E_{1/2}$ values of the Fe(II)/Fe(III) couples for difference of the arene rings in each series indicated a tendency to decrease with the number of methyl groups.

The oxidation waves were observed at ca. 800, 750 and 1400 mV for **2**, **4** or **5**, respectively, but their coupled-reduction waves were not observed, suggesting thermodynamic unstability of the oxidation products. The dppf complexes in the bridged complexes were oxidized much easily than those of the dpmf ones, suggesting that the [dpmf]$^+$ moiety has greater electron-acceptor ability than the [dppf]$^+$ one.

4. Supplementary material available

Listings of atomic coordinates, hydrogen positional parameters, isotropic and anisotropic parameters, and bond lengths and angles and tables of observed and calculated structure factors are available from the authors.

Acknowledgements

One of the authors (J.-F. Ma) was supported by a grant from Toho University.

References

[1] K.S. Gan, T.S.A. Hor, in: A. Togni, T. Hayashi (Eds.), Ferrocenes: Homogeneous Catalysis, Organic Synthesis, Material Science, VCH, Whinheim, 1995, p. 1.
[2] Y. Yamamoto, T. Tanase, I. Mori, Y. Nakamura, J. Chem. Soc. Dalton Trans. 21 (1994) 3191.
[3] (a) M.A. Bennett, M.I. Bruce, T.W. Matheson, in: G. Wilkinson, F.G.A. Stone, E.W. Abel (Eds.), Comprehenssive Organometallic Chemistry, vol. 4, Pergamon, Oxford, 1982, p. 796. (b) H. Le Bozec, D. Touchard, P.H. Dixneuf, Adv. Organomet. Chem. 28 (1989) 163.
[4] (a) Y. Yamamoto, R. Satoh, M. Ohshima, F. Matsuo, C. Sudoh, J. Organomet. Chem. 489 (1995) C68. (b) Y. Yamamoto, R. Satoh, F. Matsuo, C. Sudoh, T. Igoshi, Inorg. Chem. 35 (1996) 2329.
[5] J.-F. Ma, Y. Yamamoto, J. Organomet. Chem. 545 (1997) 577.
[6] (a) M.A. Bennett, T.-N. Huang, T.W. Matheson, A.K. Smith, Inorg. Synth. 21 (1982) 74. (b) J.W. Hull Jr., W.L. Gladfelter, Organometallics 3 (1984) 605. (c) M.A. Bennett, T.W. Metheson, G.B. Robertson, A.K. Smith, P.A. Tucker, Inorg. Chem. 19 (1980) 1014.
[7] J.J. Bishop, A. Davison, M.L. Katcher, D.W. Lichtenberg, R.E. Merrill, J.C. Smart, J. Organometal. Chem. 27 (1971) 241.
[8] D.T. Cromer, J.T. Waber, International Tables for X-ray Crystallography, vol. IV, Kynoch Press, Birmingham, UK, Table 2.2A, 1974.
[9] J.A. Ibers, W.C. Hamilton, Acta Crystallogr. 17 (1964) 781.
[10] D.C. Creagh, W.J. McAuley, in: A.J.C. Wilson (Ed.), International Tables for X-ray Crystallography, vol. C, Kluwer, Boston, MA, Table 4.2.6.8, 1992, pp. 219–222.
[11] J.G. Verkade, L.D. Quin, LD Phosphorous-31 NMR Spectoscopy in Stereochemical Analysis, VCH, Deerfield Beach, FL, 1987.
[12] (a) Y. Yamamoto, H. Yamazaki, Inorg. Chim. Acta 68 (1982) 75 and references therein. (b) F.A. Cotton, L.M. Daniels, C.A. Murillo, D.J. Timmons, Chem. Commun. (1997) 1449.
[13] F. Estevan, P. Lahuerta, J. Latorre, A. Sanchez, C. Sieiro, Polyhedron 6 (1987) 473.
[14] S. Onaka, T. Moriya, S. Takagi, A. Mizuno, H. Furuta, Bull. Chem. Soc. Jap. 65 (1992) 1415.
[15] T.S.A. Hor, H.S.O. Chan, K.-L. Tan, Y.K. Phang, L.-K. Liu, Y.-S. Wen, Polyhedron 10 (1991) 2437.
[16] L.-T. Phang, S.C.F. Au-Yeung, T.S.A. Hor, S.B. Khoo, Z.-X. Zhou, T.C.W. Mak, J. Chem. Soc. Dalton Trans. (1993) 165.
[17] T.S.A. Hor, L.-T. Phang, L.-K. Liu, Y.-S. Wen, J. Organomet. Chem. 397 (1990) 29.
[18] S. Onaka, A. Mizuno, S. Takagi, Chem. Lett. (1989) 2037.
[19] U. Casellato, D. Ajo, G. Valle, B. Corain, B. Longato, R. Graziani, J. Crystallogr. Spectrosc. Res. 18 (1988) 483.
[20] T.S.A. Hor, S.P. Neo, C.S. Tan, C.W. Mak, K.W.O. Leung, R.-J. Wang, Inorg. Chem. 31 (1992) 4510.
[21] M. Sato, M. Asai, J. Organomet. Chem. 508 (1996) 121.
[22] I.R. Butler, W.R. Cullen, R. Graziani, B. Longato, G. Pilloni, Inorg. Chem. 29 (1990) 1193.
[23] S. Onaka, Bull. Chem. Soc. Jap. 59 (1986) 2359.
[24] E.T. Singewald, C.S. Slone, C.L. Stern, C.A. Mirkin, G.P.A. Yap, L.M. Liable-Sands, A.L. Rheingold, J. Am. Chem. Soc. 119 (1997) 3048.